

Modeling Copolymer Adsorption on Laterally Heterogeneous Surfaces

Kanglin Huang and Anna C. Balazs

*Materials Science and Engineering Department, University of Pittsburgh,
Pittsburgh, Pennsylvania 15261*

(Received 6 November 1990)

We develop a self-consistent-field model for copolymer adsorption onto laterally heterogeneous surfaces. Using this model, we can predict how varying the adsorbate-surface interaction energies and the chain architecture affects the properties of polymer films on nonhomogeneous, solid interfaces. These predictions are useful in designing interfacial materials that contain ordered domains of distinct polymers and, thus, can exhibit unique electrical and optical properties.

PACS numbers: 68.15.+e, 68.35.Md, 68.45.-v, 68.55.-a

The performance of polymer coatings, polymer films, and polymer-ceramic and -metal composites depends in large part on the adsorption and adhesion of the polymers to the substrate. Substrates are commonly composed of more than one material, either through design or due to the presence of impurities. Previous theories for polymer adsorption have only described interactions with chemically uniform surfaces. Here, we introduce a self-consistent-field lattice model for copolymer adsorption onto laterally heterogeneous surfaces. Using this model, we can now undertake fundamental studies on the behavior of macromolecules at nonhomogeneous, solid interfaces. In particular, we will predict how varying the adsorbate-surface interaction energies and the chain architecture affects the structure of the polymer film.¹

We consider the surface to be composed of strips of two different materials, S1 and S2 (see Fig. 1). The solution above this substrate contains *AB* copolymers. The *A* block has an affinity for S1, while the *B* block is attracted to S2. This scenario is similar to the physical

setup in initial experimental studies of the adsorption of chainlike molecules onto surfaces that are microlithographically prepared to contain two distinct materials.² As will be shown, with *AB* diblocks in solution and at critical values of the *A*-S1 and *B*-S2 enthalpies, a strong phase segregation can be induced at the surface. That is, *A* blocks will adsorb preferentially on S1 and the *B* blocks will adsorb only on S2. However, when the molecular architecture is altered to an *AB* multiblock, this strong phase segregation can no longer be achieved.

Our model is derived from the self-consistent-field theory for polymer adsorption on flat, homogeneous surfaces developed by Scheutjens and Fleer.^{3,4} Figure 1 shows the lattice used in our new model. The $z=1$ plane represents the heterogeneous, adsorbing wall: One-half of the plane constitutes the S1 substrate, while the other half is the S2 surface. The polymer segment density is now not only a function of z (as in the previous model), but also of x . We apply a mean-field approximation only along the y direction. From the generalized Flory-Huggins equation, the potential $U_i(x,z)$ for a segment of type i in row (x,z) is given by

$$U_i(x,z) = U'(x,z) + \sum_{j(\neq i)} \chi_{ij} [\langle \phi_j(x,z) \rangle - \phi_j^b]. \quad (1)$$

The parameter $U'(x,z)$ is a "hard-core potential," which insures that every lattice row is filled. In the second term, χ_{ij} is the Flory-Huggins parameter, or the interaction energy between units i and j , and ϕ_j^b is the polymer concentration in the bulk solution. The expression $\langle \phi_j(x,z) \rangle$ is the fraction of contacts an i segment in the (x,z) row makes with j -type segments in the adjacent rows and is given by the following equation:

$$\begin{aligned} \langle \phi_j(x,z) \rangle = & \lambda_1 \phi_j(x-1,z) + \lambda_1 \phi_j(x+1,z) \\ & + \lambda_1 \phi_j(x,z-1) + \lambda_1 \phi_j(x,z+1) \\ & + \lambda_0 \phi_j(x,z), \end{aligned} \quad (2)$$

where, for a cubic lattice, $\lambda_0 = \frac{1}{3}$ and $\lambda_1 = \frac{1}{6}$. Finally, the sum over j in Eq. (1) includes interactions with other types of polymer segments and with the surfaces S1 and S2.

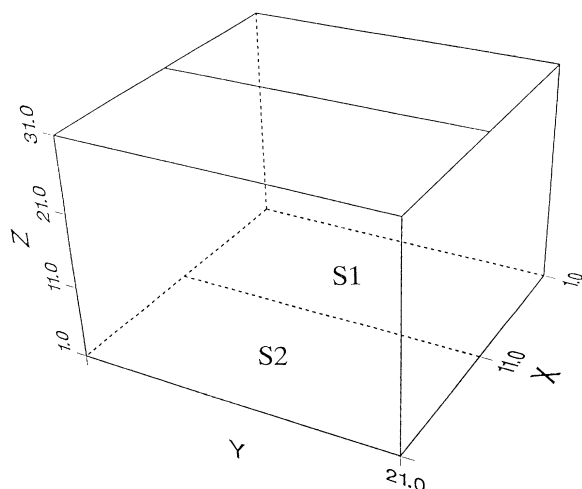


FIG. 1. An example of the three-dimensional lattice used in the calculation.

The probability that a monomer of type i is in row (x, z) with respect to the bulk is given by the factor

$$G_i(x, z) = \exp[-U_i(x, z)]. \quad (3)$$

If $G_i(x, z)$ and the solution volume fraction are known, the volume fraction is adsorbed monomers of type i is

$$\phi_i(x, z) = \phi_i^b G_i(x, z). \quad (4)$$

$$G_i(x, z, s|1) = G_i(x, z) [\lambda_1 G_i(x-1, z, s-1|1) + \lambda_1 G_i(x+1, z, s-1|1) + \lambda_1 G_i(x, z-1, s-1|1) + \lambda_1 G_i(x, z+1, s-1|1) + \lambda_0 G_i(x, z, s-1|1)]. \quad (5)$$

Clearly, $G_i(x, z, 1|1) = G_i(x, z)$ and the terms for $s > 1$ can be calculated from this relationship and Eq. (5). In the same way, we can obtain a recurrence formula for $G_i(x, z, s|r)$, the probability of a chain having its r th segment anywhere in the lattice and its s th segment in row (x, z) .

In order to obtain the volume fraction of i in row (x, z) due to segment s , in a chain of r segments, the product of two probability functions is needed: the probability of a chain starting at segment 1 and ending with segment s in row (x, z) and that of a chain starting at segment r and also ending with segment s in row (x, z) . This product must be divided by $G_i(x, z)$ in order to compensate for double counting the s segment. Hence, this volume is given by

$$\phi_i(x, z, s) = C_i G_i(x, z, s|1) G_i(x, z, s|r) / G_i(x, z), \quad (6)$$

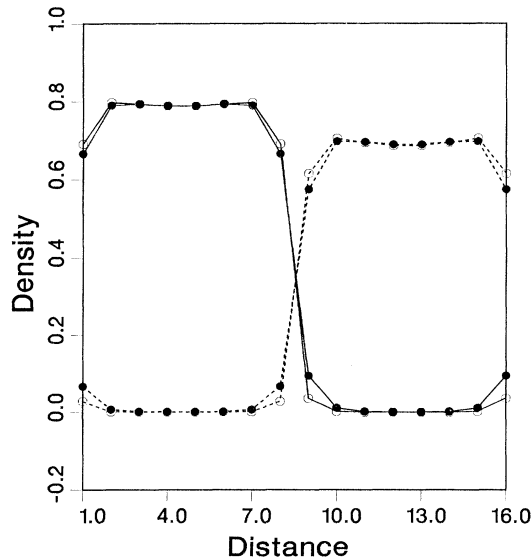


FIG. 2. The solid lines represent the volume fraction of adsorbed A in $z=2$, while the dashed lines depict the volume fraction of adsorbed B in this layer. For the curves drawn with the open circles, $\chi_{A-S1} = \chi_{B-S2} = -10$ and $\chi_{A-S2} = \chi_{B-S1} = 0$. For the curves drawn with solid circles, $\chi_{A-S1} = \chi_{B-S2} = -10$ and $\chi_{A-S2} = \chi_{B-S1} = -5$.

However, since polymers contain more than one segment, we must take into account that the segments of the chain are connected. We define $G_i(x, z, s|1)$ as the probability of a chain having its first segment anywhere in the lattice and its s th segment in row (x, z) . This function can be calculated from the following recurrence relation:

where C_i is the normalization constant and is equal to ϕ_i^b / r_i . The total volume fraction $\phi_i(x, z)$ of molecules i in row (x, z) can be obtained by summing over s :

$$\phi_i(x, z) = \sum_{s=1}^r \phi_i(x, z, s). \quad (7)$$

From Eqs. (1), (6), and the condition that $\sum_i \phi_i(x, z) = 1$ for each row, the adsorption profile can be calculated through standard numerical techniques.

We note that the equations derived above are related to the recent calculations describing the behavior of lipid bilayers.⁵

Periodic boundary conditions are applied along the y direction of the box. A specific example of this box is given in Fig. 1. In the calculations presented here, χ_{AB} is set equal to 0.5. The surface-solvent interaction energy is set equal to 0.0 for both S1 and S2. The length of the AB copolymer is 50 lattice sites: 25 sites are A 's and 25 sites are B 's.

Figure 2 shows the polymer density in the layer directly above the surface, the $z=2$ layer, versus distance along the x direction of the surface. The region on the left, or $x=1-8$, represents the S1 domain and $x=9-16$ represents the S2 region. The solid curves describe the volume fraction of the A molecules in the $z=2$ layer, while the dashed curves represent the volume fraction of B molecules in this layer. The curves drawn with open circles describe the experiment in which χ_{A-S1} and χ_{B-S2} were both set equal to -10 , while $\chi_{A-S2} = \chi_{B-S1} = 0$. The interaction energy between A and the solvent is equal to 0.5, while the interaction between B and the solvent is equal to 0. Thus, the solution is a poor solvent for the A moiety, but an athermal solvent for the B block. As can be seen, due to the strong affinities for the respective surfaces, the copolymers bind with the A segments strongly segregated to the S1 domain and "upside down" with the B blocks strongly localized on the S2 region. (Since the B segments are not repelled from the solvent, there is slightly less of the B blocks adsorbed onto the interface.)

In a second experiment, χ_{A-S1} and χ_{B-S2} were held fixed at -10 ; however, $\chi_{A-S2} = \chi_{B-S1}$ were set equal to -5 . Now, there is a finite attraction between the A 's and the S2 plane and the B 's and the S1 region. The result-

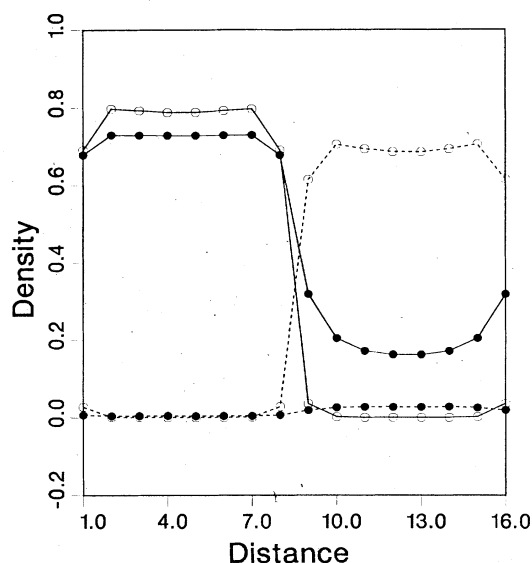


FIG. 3. For the curves drawn with the open circles, $\chi_{A-S1} = \chi_{B-S2} = -10$ and $\chi_{A-S2} = \chi_{B-S1} = 0$, as above. For the curves drawn with solid circles, $\chi_{A-S1} = -10$, $\chi_{A-S2} = -5$, and $\chi_{B-S1} = \chi_{B-S2} = 0$.

ing curves are essentially identical to the open-circle lines, except at the boundary between the two regions (see Fig. 2). Here, the small concentration of A on $S2$ in $x=9$ (and similarly, the amount of B on $S1$ in $x=8$) is nonetheless twice as high as in the previous experiment. [Correspondingly, the amount of A in $x=8$ (and the amount of B in $x=9$) is slightly depressed from the previous values.] Even though the A 's have an affinity for $S2$, these blocks are excluded from all but the edges of the region by the more strongly attracted B 's. In the same manner, the B 's are excluded from the interior of $S1$.

In a third experiment, χ_{A-S1} was held fixed at -10 and χ_{A-S2} was also maintained at -5 ; however, χ_{B-S2} and χ_{B-S1} were both set equal to zero. These results are drawn as a line containing solid circles in Fig. 3. The A 's are still attracted to the $S1$ domain; thus, there is a high concentration of A in this region. However, the B 's are no longer attracted to the surface; thus, very few B blocks actually bind to the interface. Consequently, the A blocks, which also have an affinity to $S2$, can now bind onto this domain; they are no longer excluded from the region by the competitive adsorption of the B blocks. As can be seen, the clean segregation of the chains onto the respective domains is now destroyed.

In a final experiment, we set $\chi_{A-S1} = \chi_{B-S2} = -10.0$ and $\chi_{A-S2} = \chi_{B-S1} = 0.0$, as in the first trial; however, we altered the copolymer geometry from a diblock to an alternating multiblock. In particular, a block of five A sites lies next to a block of five B sites along the length of

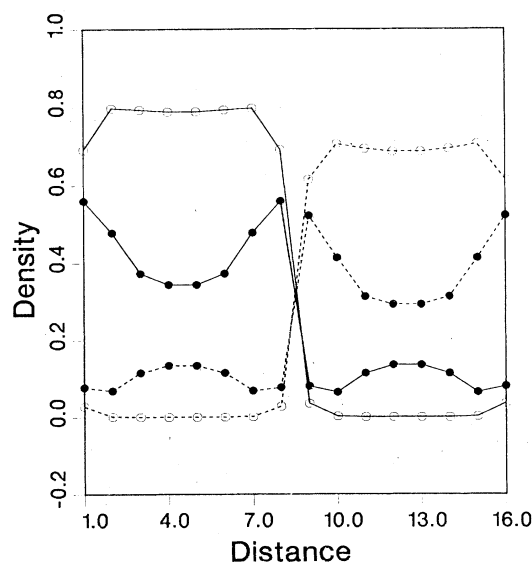


FIG. 4. For the curves drawn with open circles, $\chi_{A-S1} = \chi_{B-S2} = -10$ and $\chi_{A-S2} = \chi_{B-S1} = 0$ and the copolymer has a diblock architecture. For the curves drawn with solid circles, all the χ 's are the same as above; however, the chain now has a multiblock structure.

the fifty-site chain. The polymer density in the $z=2$ layer for this case is given in Fig. 4. Even though the A 's are not attracted to $S2$, there is a finite concentration of these species in the interior of the $S2$ domain. The presence of these species is due to the fact that they are dragged down onto the surface by the B 's that neighbor this block on both sides and that are, in fact, strongly attracted to the $S2$ domain. The same phenomenon can account for the presence of B 's in the $S1$ region. Now, the specific polymer architecture prohibits the possibility of a complete segregation of the A 's on one domain and the B 's on the other.

In conclusion, we have developed a model to investigate the adsorption of copolymers onto laterally heterogeneous surfaces. The equilibrium properties of these chains depend not only on the relevant interaction energies, but also on the polymer architecture. For diblock copolymers, the values of χ_{A-S1} and χ_{B-S2} are the most important in controlling the localization of the chains onto the respective domains. For sufficiently attractive energies, a complete segregation of the two blocks on the surface can be induced. However, by altering the copolymer architecture, this surface segregation can be destroyed.

These predictions are useful in designing interfaces that contain well-defined, ordered domains of different macromolecules. Such materials can be tailored to display unique electrical and optical properties, which can be used in a variety of technological applications.

A.C.B. gratefully acknowledges financial support from

NSF, through Grant No. DMR-8718899.

¹K. Huang and A. C. Balazs, in Proceedings of American Chemical Society, Polymer Chemistry Division, Atlanta, 14-17 April 1991 (to be published).

²P. E. Laibinis, J. J. Hickman, M. S. Wrighton, and G. M.

Whitesides, *Science* **245**, 845 (1989).

³J. M. H. M. Scheutjens and G. J. Fleer, *J. Phys. Chem.* **83**, 1619 (1979).

⁴O. A. Evers, J. M. H. M. Scheutjens, and G. J. Fleer, *J. Chem. Soc. Faraday Trans.* **86**, 1333 (1990).

⁵F. A. M. Leermakers, J. H. M. Scheutjens, and J. Lyklema, *Biochim. Biophys. Acta* **1024**, 139 (1990).